Purely STDP-based assembly dynamics: stability, learning, overlaps, drift and aging

Paul Manz [1], Raoul-Martin Memmesheimer [1,*],

1 Neural Network Dynamics and Computation, Institute of Genetics, University of Bonn, Bonn, Germany

* rm.memmesheimer@uni-bonn.de

Abstract

Memories may be encoded in the brain via strongly interconnected groups of neurons, called assemblies. The concept of Hebbian plasticity suggests that these assemblies are generated through synaptic plasticity, strengthening the recurrent connections within select groups of neurons that receive correlated stimulation. To remain stable in absence of such stimulation, the assemblies need to be self-reinforcing under the plasticity rule. Previous models of such assembly maintenance require additional mechanisms of fast homeostatic plasticity often with biologically implausible timescales. Here we provide a model of neuronal assembly generation and maintenance purely based on spike-timing-dependent plasticity (STDP) between excitatory neurons. It uses irregularly and stochastically spiking neurons and STDP that depresses connections of uncorrelated neurons. We find that assemblies do not grow beyond a certain size, because temporally imprecise spike correlations dominate the plasticity in large assemblies. Assemblies in the model can be learned or spontaneously emerge. The model allows for prominent, stable overlap structures between static assemblies. Further, assemblies can drift, particularly according to a novel, transient overlap-based mechanism. Finally the model indicates that assemblies grow in the aging brain, where connectivity decreases.

Author summary

It is widely assumed that memories are represented by ensembles of nerve cells that have strong interconnections with each other. It is to date not clear how such strongly interconnected nerve cell ensembles form, persist, change and age. Here we show that already a basic rule for activity-dependent synaptic strength plasticity can explain the learning or spontaneous formation and the stability of assemblies. In particular, it is not necessary to explicitly keep the overall total synaptic strength of a neuron nearly constant, a constraint that was incorporated in previous models in a manner inconsistent with current experimental knowledge. Furthermore, our model achieves the challenging task of stably maintaining many overlaps between assemblies and generating the experimentally observed drift of memory representations. Finally, the model predicts that when the number of synaptic connections in the brain decreases, as observed during aging, the size of the neuron ensembles underlying memories increases. This may render certain memories in the aging brain more robust and prominent but also less specific.

Introduction

A widely used model of long-term memory posits that items are stored in the brain by strongly interconnected neuronal assemblies [1–3]. A memory item is represented by a group of neurons that coactivate upon memory recall. The assembly structure allows for associative recall from an incomplete input: due to the strong interconnections, activation of a part of the neurons in an assembly can trigger reactivation of the entire assembly and thus a recall of the full memory. The assemblies may each be created through experience-dependent plasticity or they may already form during development [4]. In the latter case, memories may form by connecting the pre-existing assemblies to appropriate input and output neurons [5]. The theory of the formation and maintenance of neuronal assemblies has been studied in much detail in previous works. The creation of new memories is commonly modeled using Hebbian plasticity [6–13]: if a set of neurons is co-activated, Hebbian plasticity increases the strength of their mutual connections leading to the formation of what is called a Hebbian assembly. However, memory networks in the brain also show ongoing spontaneous and irregular activity. If plasticity still takes place during this activity, it should not interfere with the existing memory assemblies – otherwise memories would have implausibly short lifespans. Hebbian assemblies can be self-reinforcing under plasticity since their interconnectedness leads to higher correlations in the activities, which in turn leads to potentiation of the intra-assembly weights. Models of assembly maintenance, however, found that fast homeostatic plasticity was needed in addition to Hebbian learning. This introduces competition between synapses and prevents pathological growth of assemblies and exploding activity [5, 7–9, 11–13]. Homeostatic plasticity has been observed in experiments, but it is much slower than Hebbian plasticity and does therefore not suffice to prevent runaway potentiation [14–18] (see, however, [19] for a different view and [10, 20] for a small timescale implementation of homeostasis via inhibitory STDP).

Experiments indicate that distinct memory assemblies have a fraction of shared neurons, i.e. neurons that are part of both assemblies [21–23]; the size of these overlaps appears to correspond to the strength of the associations between the concepts encoded by the assemblies. Previous models of assemblies stabilized by recurrent synaptic plasticity and fast homeostatic normalization usually do not show prominent overlaps [5, 7–9, 12]. An example of a network with weight plasticity, structural plasticity, multiple synapses per connection and short-term depression that can store two strongly overlapping assemblies was given in [24]. We will explore whether our purely STDP-based model can maintain overlaps.

Another topic of interest in the study of memory networks is whether they can generate the representational drift observed in recent experiments [25]. Such drift has recently been modeled by drifting assemblies, which spontaneously exchange neurons with each other, leading to a gradual resorting of the whole network [5]. The network model incorporated fast homeostatic normalization to stabilize the assemblies. We will explore whether also our purely STDP-based model can exhibit drifting assemblies.

Finally, many conditions, such as aging are associated with a decrease in overall connectivity [26, 27]. We will therefore explore how the assemblies in our networks adapt to such a decrease.

The paper is structured as follows: We initially introduce the model of spiking neurons and STDP and describe existing analytical approximations for the time-averaged weight dynamics. As a first result, we show spontaneous assembly formation. We then obtain an analytical approximation of the weight growth in different assembly sizes to obtain an understanding of the numerically observed assembly formation. Next we study whether assemblies can be learned by correlated external input. The subsequent section shows that our networks can stably maintain

overlapping assemblies. We then examine whether our model can be set up to exhibit representational drift. Finally, we investigate the dependence of assembly sizes on network sparsity and relate our results to effects of aging on the brain.

Materials and methods

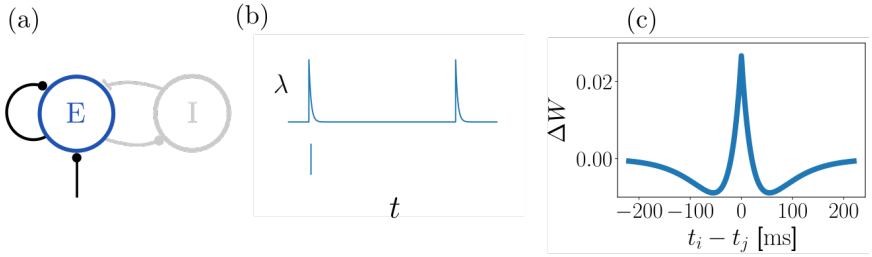

Fig 1. Network, neuron and plasticity model. (a): A network consists of recurrently connected excitatory neurons, which generate irregular, stochastic spiking. It may be interpreted as the excitatory population of a neural network where excitatory and inhibitory neurons generate a balanced state [28] of irregular spiking. Thus, an inhibitory neuron population is implicitly contained in our model. (b): Poisson model of stochastic single neuron spiking: each neuron is characterized by its instantaneous rate $\lambda(t)$ (upper subpanel), which depends on incoming spikes and determines the probability of emitting a spike (lower subpanel). (c): Strength of STDP updates as a function of the time difference between pre- and postsynaptic spikes for $\mu = 1$.

Poisson neurons

Neural networks in the mammalian brain typically generate irregular and apparently largely stochastic spiking. To guarantee that our model networks generate similar spiking activity, we consider networks of stochastic linear Poisson (or "Hawkes") model neurons [9, 29–31]. Such networks are additionally analytically well tractable. We explicitly model excitatory neurons. Since the irregular activity in biological neural networks is likely due to a balanced state, where excitatory and inhibitory inputs to each neuron balance [28, 32–36], our model implicitly incorporates inhibitory neurons, see Fig. 1.

The spiking activity of each neuron i is an inhomogeneous Poisson process whose time-dependent instantaneous spike rate (intensity) $\lambda_i(t) = \langle S_i(t) \rangle$ given input spike trains $S_k(t) = \sum_m \delta(t - t_k^m)$ up to time t and weights W_{ik} is

$$\lambda_i(t) = \lambda_i^0 + \sum_k W_{ik} \sum_m a(t - t_m^k). \tag{1}$$

The angular brackets here denote trial-averaging with fixed input spike trains and weights to neuron i. We use an exponentially decaying synaptic kernel

$$a(t) = \frac{\Theta(t)}{\tau_s} \mathrm{e}^{-\frac{t}{\tau_s}}, \tag{2}$$

where $\Theta(t)$ is the Heaviside distribution, and a constant external drive λ^0.

It is now useful to introduce quantities that are trial-averaged over the entire spiking network dynamics. The trial-averaged instantaneous rate (intensity) of neuron i is $r_i(t) = \langle \lambda_i(t) \rangle$, where angular brackets now denote the trial-averaging over the network

dynamics. For static W with spectral radius less than 1, the trial-averaged rate dynamics relax to a fixed point where the vector $r(t)$ is constant,

$$r = (\mathbb{1} - W)^{-1} \lambda^0, \tag{3}$$

see [9, 30, 37, 38]. In addition, one can analytically compute the corresponding stationary cross-correlation functions $C_{ij}(\tau) = \langle S_i(t+\tau) S_j(t) \rangle$ of pairs of neurons i, j at arbitrary t; in the frequency domain they read

$$\tilde{C}(\omega) = 2\pi\delta(\omega) r r^T + \left(\mathbb{1} - \tilde{a}(\omega) W\right)^{-1} D \left(\mathbb{1} - \tilde{a}(-\omega) W^T\right)^{-1}, \tag{4}$$

where we used matrix notation and $D_{ij} = \delta_{ij} r_i$ [9, 30, 38]. The Fourier transform of a function $g(t)$ is defined as $\tilde{g}(\omega) = \int_{-\infty}^{\infty} \mathrm{d}t \mathrm{e}^{-i\omega t} g(t)$. If the scale of the STDP updates is sufficiently small, one can assume that the weight dynamics are quasistationary with respect to neuronal dynamics. Then Eqs. 3,4 still approximately hold true despite W changing over time due to plasticity.

Spike-timing-dependent plasticity

We consider networks of spiking neurons with pair-based STDP, i.e. the change of synaptic strength depends on the time lags of pairs of pre- and postsynaptic spikes. The characteristics of the plasticity function crucially determine how synaptic strengths evolve in a network. Networks with symmetric plasticity functions can establish a structure of neuronal assemblies whereas plasticity functions with a large antisymmetric part tend to establish feedforward chains of connectivity; see, however, [10, 20] for networks with asymmetric STDP maintaining assemblies and [12] for a triplet STDP rule that forms assemblies despite an asymmetric two-spike interaction part. In the present work, we consider symmetric plasticity functions because of their simplicity and analytical tractability, building on previous theoretical work that has employed them [5, 9]. Symmetric STDP has been found in the CA3 region of the rodent hippocampus [39], i.e. in a region that is assumed to serve as an associative memory network and to store assemblies [1]. Recently, near-symmetric STDP has also been observed in the primary motor cortex of primates [40].

The change induced by a spike pair with time lag t is given by the STDP function F,

$$F(t) = \mu \left(A_\mathrm{p} \mathrm{e}^{-\frac{|t|}{\tau_p}} + A_\mathrm{d} \mathrm{e}^{-\frac{|t|}{\tau_d}} \right), \tag{5}$$

where the scaling factor μ is the learning rate, $A_\mathrm{p} > 0$, $A_\mathrm{d} < 0$, $|A_\mathrm{p}| > |A_\mathrm{d}|$ and $\tau_\mathrm{p} < \tau_\mathrm{d}$, see Fig. 1c. For the analytical treatment of our plasticity rule we set $\mu = 1$. In all our simulations the parameters are chosen such that the integral $\int_{-\infty}^{\infty} \mathrm{d}t\ F(t)$ over F is negative.

At each spike time, plasticity acts additively on the pre- and postsynaptic weights of the spiking neuron, with amplitudes given by F. Specifically, at a spike time t_{k_i} of the postsynaptic neuron there is a jump-like change in W_{ij} of $\sum_{t_{k_j} \le t_{k_i}} F(t_{k_i} - t_{k_j})$. At a spike time t_{j_k} of the presynaptic neuron W_{ij} jumps by $\sum_{t_{k_i} \le t_{k_j}} F(t_{k_i} - t_{k_j})$. This can be compactly written as

$$\frac{\mathrm{d}}{\mathrm{d}t} W_{ij}(t) = \sum_{t_{k_i}, t_{k_j} \le t} \left(F(t_{k_i} - t_{k_j}) \delta(t - t_{k_i}) + F(t_{k_i} - t_{k_j}) \delta(t - t_{k_j}) \right). \tag{6}$$

Here and henceforth we assume $i \neq j$; there is no self-interaction in our networks, $W_{ii} = 0$. We further stipulate that no weight can become negative or exceed a maximum

value $\hat{w}$ due to STDP: if a synapse would be depressed below 0 it will be set to 0 instead and if a synapse would be potentiated to a value beyond $\hat{w}$ it will be set to $\hat{w}$.

In the regime of quasistationary weight dynamics the time-averaged drift in synaptic efficacy, $\overline{\Delta W_{ij}}$, can be approximated by

$$\overline{\Delta W_{ij}} := \frac{1}{T}\int_t^{t+T} \mathrm{d}t' \; \frac{\mathrm{d}}{\mathrm{d}t'} W_{ij}(t') = \int_{-\infty}^{\infty} \mathrm{d}\tau \; C_{ij}(\tau) F(\tau), \tag{7}$$

where $C_{ij}(\tau)$ are again the correlations of the spike trains of neurons i and j [29]. Plancherel's theorem then yields

$$\overline{\Delta W_{ij}} = \frac{1}{2\pi}\int_{-\infty}^{\infty} \mathrm{d}\omega \; \tilde{C}_{ij}(\omega)\tilde{F}(-\omega), \tag{8}$$

with the Fourier transforms of the correlation function and of the STDP window. Inserting the correlation function $\tilde{C}_{ij}(\omega)$ of Eq. 4 gives

$$\begin{aligned}\overline{\Delta W_{ij}} &= f_0 r_i r_j \\ &+ \frac{1}{2\pi}\int_{-\infty}^{\infty} \mathrm{d}\omega \; \sum_k \left[(\mathbb{1} - \tilde{a}(\omega)W)^{-1}\right]_{ik} r_k \left[(\mathbb{1} - \tilde{a}(-\omega)W^T)^{-1}\right]_{kj} \\ &\qquad \times \tilde{F}(-\omega),\end{aligned} \tag{9}$$

see [9], where

$$f_0 = \tilde{F}(0) = \int_{-\infty}^{\infty} \mathrm{d}t \; F(t) = 2\left(A_\mathrm{p}\tau_\mathrm{p} + A_\mathrm{d}\tau_\mathrm{d}\right). \tag{10}$$

It is often useful to expand Eq. 4 into a power series with respect to W [30]. Inserting the series into the right hand side of Eq. 8 (or directly expanding Eq. 9) results in a series expansion for $\overline{\Delta W_{ij}}$, [9]:

$$\overline{\Delta W_{ij}} = f_0 r_i r_j + \sum_{\alpha,\beta} f_{\alpha\beta} \sum_m r_m (W^\alpha)_{im} (W^\beta)_{jm}. \tag{11}$$

The terms of the sum encode contributions from motifs in which a source neuron affects post- and presynaptic neurons via a chain of α and β connections, respectively (the same connection may be counted more than once). If $\alpha = 0$ ($\beta = 0$) the post(pre)synaptic neuron itself is the source. The coefficients $f_{\alpha\beta}$ contain integrals over the Fourier transform of the STDP window and powers of the Fourier transform of the synaptic kernel function,

$$f_{\alpha\beta} = \frac{1}{2\pi}\int_{-\infty}^{\infty} \mathrm{d}\omega \; \tilde{F}(-\omega)\tilde{a}(\omega)^\alpha \tilde{a}(-\omega)^\beta. \tag{12}$$

Results

Spontaneous assembly formation

We first simulate the model described above with initially unstructured weight matrix and without structured external stimulation, in order to test its capability of spontaneous assembly formation and subsequent maintenance. We find that for appropriately chosen parameters in the plasticity function the network weights indeed converge towards a structure with segregated assemblies of a characteristic size.

The mechanism underlying the increase of weights between assembly neurons is well known: Initially basically randomly coincident spiking leads to strengthening of some weights. These weights induce more near-simultaneous spiking, which further strengthens them. The positive feedback loop leads to weights that increase until they reach $\hat{w}$ [41]. It has been shown that if the summed weight strength to and from a neuron are additionally normalized by fast homeostasis, there can be spontaneous emergence of assemblies [5, 9, 12, 13]. The reason is that the homeostatic normalization lets synapses compete, such that more slowly growing ones are suppressed. Once an imbalance of connectivity and thus first assembly-like structures occur, the weight increase of intra-assembly synapses prior to normalization is stronger, due to the stronger co-spiking of the connected neurons. The normalization then suppresses the inter-assembly connections and the assembly structure consolidates.

In our networks, there is no fast homeostatic normalization that could introduce competition between synapses. Then, why do not all weights tend to $\hat{w}$? In other words: why does the network not turn into one big assembly?

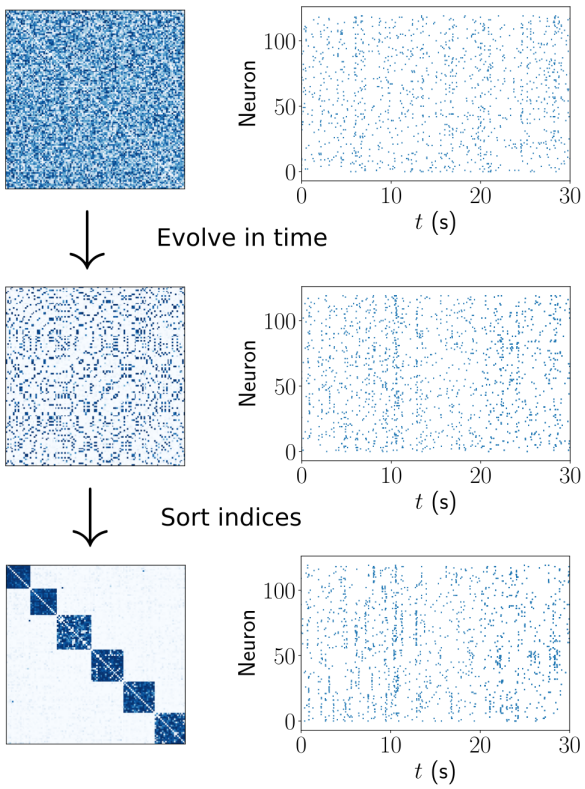

Fig 2. Spontaneous assembly formation. Several assemblies (strongly interconnected ensembles of neurons) emerge in a network with initially random connectivity, due to spontaneous activity.

Plasticity in homogeneously connected assemblies

In this section, we will argue that the assembly growth is in our model limited because of the depression dominance of the learning rule. For this we consider the special case of an isolated assembly of N neurons that is homogeneously connected with synaptic strengths $\hat{w}$. We compute $\overline{\Delta W_{ij}}$ for weights within this type of assembly, disregarding

the clipping at $\hat{w}$. This indicates whether and how vigorously weights that fall below $\hat{w}$ are restored towards it. Further, it indicates how successfully further neurons are recruited, as recruitment relies on increasing the weights to new neurons once they are randomly increased. Since assemblies compete for neurons, we therefore expect the preferred assembly size to be the one that maximizes $\overline{\Delta W_{ij}}$.

To analytically obtain $\overline{\Delta W_{ij}}$ as a function of the assembly size, we first compute from Eq. 3 the average rate of an assembly neuron

$$r = \lambda_0 \sum_{m=0}^{\infty} ((N-1)\hat{w})^m = \frac{\lambda_0}{1-(N-1)\hat{w}} = \frac{\lambda_0}{1-\rho}, \tag{13}$$

where $\rho = (N-1)\hat{w}$ is the branching parameter, which gives the average number of spikes that are directly induced by a single spike in the assembly. A stable network requires $\rho < 1$ [31, 42, 43]. Eqs. 4, 13 and 8 yield

$$\begin{aligned}\overline{\Delta W_{ij}}(N) = &\frac{2\lambda_0^2(A_\mathrm{p}\tau_\mathrm{p} + A_\mathrm{d}\tau_\mathrm{d})}{(1-(N-1)\hat{w})^2} + \\ &+ \frac{\lambda_0 A_\mathrm{p}\tau_\mathrm{p}\hat{w}\left[(2-(N-2)\hat{w})\tau_\mathrm{p} + (2-(N-2)\hat{w} - (N-1)\hat{w}^2)\tau_\mathrm{s}\right]}{(1+\hat{w})(1-(N-1)\hat{w})^2(\tau_\mathrm{s} + (1+\hat{w})\tau_\mathrm{p})(\tau_\mathrm{s} + (1-(N-1)\hat{w})\tau_\mathrm{p})} + \\ &+ \frac{\lambda_0 A_\mathrm{d}\tau_\mathrm{d}\hat{w}\left[(2-(N-2)\hat{w})\tau_\mathrm{d} + (2-(N-2)\hat{w} - (N-1)\hat{w}^2)\tau_\mathrm{s}\right]}{(1+\hat{w})(1-(N-1)\hat{w})^2(\tau_\mathrm{s} + (1+\hat{w})\tau_\mathrm{d})(\tau_\mathrm{s} + (1-(N-1)\hat{w})\tau_\mathrm{d})},\end{aligned} \tag{14}$$

see SI S.1 for details. Assuming that $N \gg 1$, we can neglect N's discrete nature and consider the limit where it approaches $1 + \frac{1}{\hat{w}}$. In this limit, the firing rates diverge and Eq. 14 gives

$$\begin{aligned}&\lim_{N\to 1+\frac{1}{\hat{w}}} \overline{\Delta W_{ij}}(N) \\ &= \lim_{N\to 1+\frac{1}{\hat{w}}} \left(\frac{2\lambda_0^2(A_\mathrm{p}\tau_\mathrm{p} + A_\mathrm{d}\tau_\mathrm{d})}{(1-(N-1)\hat{w})^2} + \frac{\lambda_0\hat{w}\left(A_\mathrm{p}\tau_\mathrm{p} + A_\mathrm{d}\tau_\mathrm{d}\right)}{\tau_\mathrm{s}(1+\hat{w})(1-(N-1)\hat{w})^2} \right) \qquad (15) \\ &= \lim_{N\to 1+\frac{1}{\hat{w}}} f_0 \left(\frac{\lambda_0^2}{(1-(N-1)\hat{w})^2} + \frac{\lambda_0\hat{w}}{2\tau_\mathrm{s}(1+\hat{w})(1-(N-1)\hat{w})^2} \right), \qquad (16)\end{aligned}$$

where we used Eq. 10 to obtain the last line. It implies

$$\lim_{N\to 1+\frac{1}{\hat{w}}} \overline{\Delta W_{ij}}(N) = -\infty \text{ if } f_0 < 0, \tag{17}$$

since the summands in the large bracket are positive. Thus, if $f_0 < 0$ and there is an N for which $\overline{\Delta W_{ij}}(N)$ is positive, $\overline{\Delta W_{ij}}(N)$ will have a maximum; we therefore expect limited assembly growth and assume $f_0 < 0$ throughout the article. Indeed, if $f_0 > 0$, $\overline{\Delta W_{ij}}(N)$ diverges to positive values for N where also the firing rate diverges, indicating that sufficiently large assemblies continue to grow until the network generates pathological activity.

The first term in the bracket of Eq. 16 covers the impact of uncorrelated pre- and postsynaptic spiking with rates r_j and r_i on the synaptic strengths ($C_{ij}(\tau) = r_i r_j$ for uncorrelated spiking). As the firing rates increase with N, the contribution of the STDP rule due to uncorrelated spiking tends to increasingly negative values, since $f_0 < 0$. The fact that the second term, which encodes the effects of connectivity motifs on STDP, see Eq. 11, also becomes negative for sufficiently large N is due to contributions from higher order motifs. We can see this by reconsidering Eq. 11: For

homogeneously connected assemblies, it simplifies to

$$\overline{\Delta W_{ij}} = f_0 r^2 + \frac{r}{N} \sum_{\alpha+\beta>0} f_{\alpha\beta} \left((N-1)^{\alpha+\beta} - (-1)^{\alpha+\beta} \right) \hat{w}^{\alpha+\beta} \tag{18}$$

$$= f_0 r^2 + \frac{r}{N} \sum_{k=1}^{\infty} f_k \left((N-1)^k - (-1)^k \right) \hat{w}^k, \tag{19}$$

where

$$f_k := \sum_{\alpha+\beta=k} f_{\alpha\beta}, \tag{20}$$

see SI S.2. Since $f_{\alpha\beta}$ (cf. Eq. 12) and thus f_k are independent of N, higher order terms in k grow in Eq. 19 faster with N than lower order ones. Therefore higher order motifs become more relevant for the weight change the larger N is. We find for high orders that

$$\lim_{k\to\infty} f_k = \frac{f_0}{2\tau_s}, \tag{21}$$

see SI S.2; therefore high order motifs induce synaptic depression.

Importantly, the relation Eq. 21 holds generally, for any plasticity window F, not only for the considered symmetric one. We explain it as follows: A term with specific exponents α and β in Eqs. 11, 18 covers the contribution of a specific connectivity motif to the spike correlation. This motif consists of a common presynaptic neuron that is separated from neurons j and i by a chain of β and α connections, respectively [9], see Fig. 3b for an illustration. Higher orders of $k = \alpha + \beta$ thus encode the effects of long cascades of spiking activity in an assembly. The longer these cascades get, the more spread-out and Gaussian the temporal distribution of their impacts becomes, due to the summation of inter-spike-intervals and their jitters. (We note that since the considered model is linear, one can indeed attribute the generation of each spike to a precursor spike or to the external drive.) Eq. 20 homogeneously sums over motifs with different connection chain lengths to the pre- and the postsynaptic neuron. For sufficiently large k the evoked spike time differences are thus equidistant, broad, overlapping Gaussians over the STDP window, which leads to the dependence on the integral of the STDP function f_0, as for uncorrelated pre- and postsynaptic spiking.

Fig. 3a shows $\overline{\Delta W_{ij}}(N)$ as in Eq. 14 for different values of $\hat{w}$: $\overline{\Delta W_{ij}}(N)$ is maximal for a particular assembly size and becomes negative for large assembly sizes. We confirmed these results using simulations of homogeneous assemblies, in which the weight updates that would occur due to STDP without clipping are tracked but not applied and then averaged over time. Further, Fig. 2 confirms the idea that the observed assembly sizes are roughly at the maximum of $\overline{\Delta W_{ij}}(N)$: the first two assemblies that emerged in Fig. 2 consist of 16 and 18 neurons, respectively, which is roughly where the maximum of the corresponding curve in Fig. 3 is ($\hat{w} = 0.40$).

We note that in our simulations we also find sparser assemblies where some internal connections are weak or basically missing. For these we expect the maximum of $\overline{\Delta W_{ij}}$ to be at larger sizes compared to our estimates with fully connected ones. Consistent with this, we observe that sparser assemblies in our simulations tend to be larger.

Storing new assemblies

Next we show how assemblies can be learned via correlated feedforward input. Neurons recruited for a new assembly may previously have only weak connections, i.e. they may belong to a background of neurons in front of which assemblies exist. Alternatively recruited neurons may already be part of other assemblies. In our simulations, during the learning phase, each neuron that is to be recruited receives Poisson spike input from

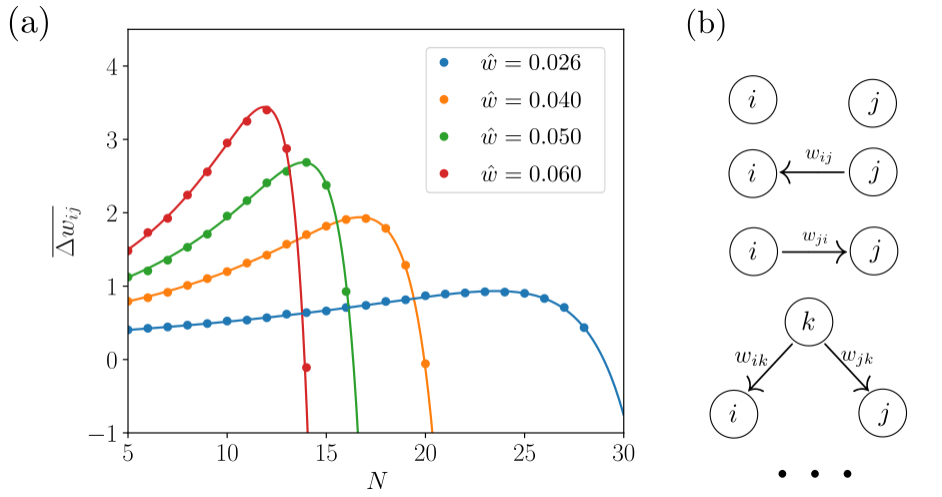

Fig 3. Explanation of assembly formation. (a): Time-averaged weight change (tracked, not applied; arbitrary units) for a synapse in an assembly (fully connected, no other connections, all weights fixed at $\hat{w}$) as a function of its size N, for different values of $\hat{w}$. Solid lines: theoretical prediction. (b): Illustration of zeroth, first and second order contributions to the time-averaged weight change for a given rate and weight configuration.

the same source. This stimulates the neurons to spike near-simultaneously, such that the weights between them grow. Fig. 4 displays the resulting weight and spiking dynamics in a network which prior to stimulation hosts one assembly in front of a background of weakly coupled neurons. Before time $t = 0$s, the single assembly is stably stored in the network, despite the ongoing plasticity. At $t = 0$ s a group of background neurons receives correlated stimulation for $T_{\text{stim}} = 180$ s. This leads to the formation of a rudimentary assembly. After the stimulation has ended, its synapses grow over a longer period of time until a fully connected assembly is reached, where all interconnections have synaptic strength close to $\hat{w}$. The remaining background neurons, which do not receive correlated stimulation in the beginning, do not form assemblies. The stimulation furthermore does not affect the already existing assembly and neither does this assembly interfere with the formation of the new assembly. Fig. S2 shows another example of assembly learning; here again mostly background neurons are recruited, but also one neuron that is already part of two pre-existing assemblies.

Overlapping Assemblies

Experiments indicate that neurons can code for more than one memory item [21–23]. For assembly models of memory this implies that neurons can be part of more than one assembly, see Fig. 5a, i.e. assemblies have overlaps [44]. Such overlaps may encode associations between memories.

We find that for appropriate parameters, our networks can stably store assemblies with some overlaps, see Fig. 5b for an example weight matrix. However, we also observe that overlapping assemblies present a challenge for our models: overlapping assemblies either tend to merge or overlapping neurons tend to disconnect from one of the assemblies they are a part of, dissolving the overlap. The first case occurred especially when the sizes of the overlapping assemblies were significantly smaller than the sizes that would maximize $\overline{\Delta W_{ij}}$. We hypothesize that in this case a feedback loop emerges: overlaps induce correlations between the assemblies, which facilitates the formation of

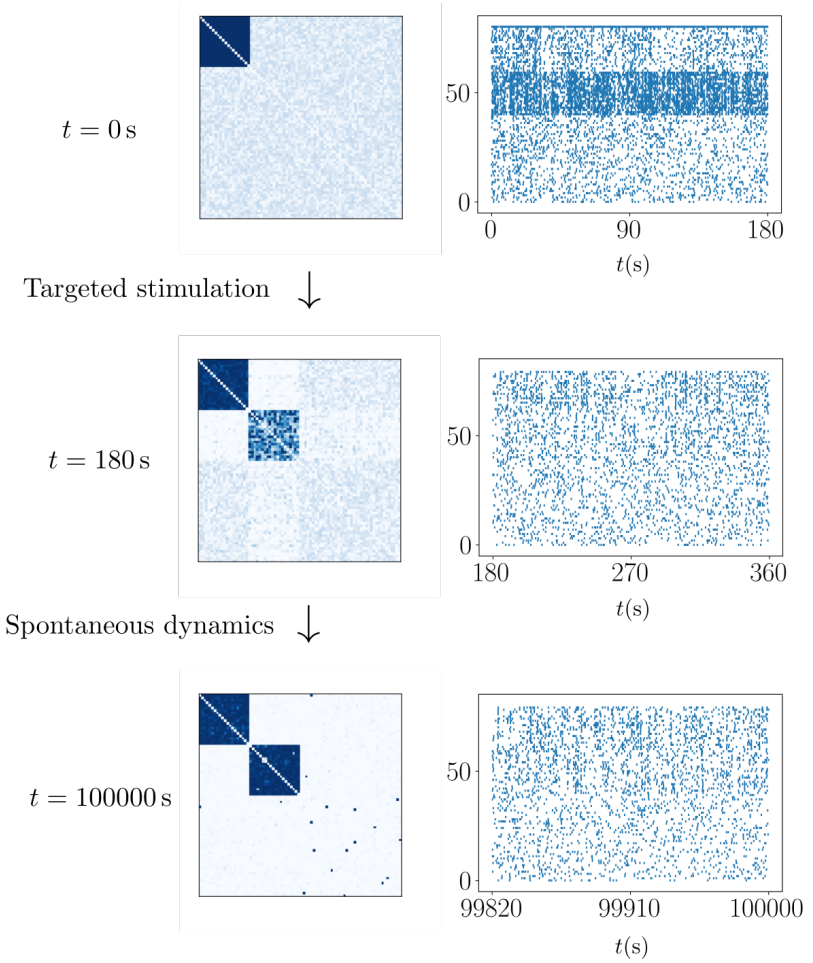

Fig 4. Learning a new assembly in a network starting with a single assembly and otherwise weak random connectivity. Initially, correlated external input stimulates the neurons of the new assembly, which leads to an increase of their interconnecting weights and thereby to the formation of a rudimentary assembly. The stimulation is then turned off and the network evolves on its own; the new assembly becomes fully connected.

additional overlaps until the assemblies have completely fused. The other case occurred when the sizes of the two assemblies were close to maximizing $\overline{\Delta W_{ij}}$. We hypothesize that here the higher firing rate of an overlap neuron and the resulting increased negative contribution (from, for example, the first term in Eq. 14) imply that overlaps become more likely to disappear due to fluctuations in the weight dynamics.

The hypotheses about the mechanism underlying the problems with overlap suggest two solutions how networks may solve them: First, if the synaptic long-term depression that occurs at high rates limits the connectivity of neurons, a neuron with a significantly lower spontaneous rate may be able to connect to multiple assemblies at the same time. In Fig. 6 we show how neurons with lower spontaneous firing rate join a second assembly. In Fig. 6a a neuron with lowered spontaneous rate is already partially connected to another assembly. This partial connection then causes enough correlation with the second assembly to induce the completion of the connections. In this case both the initial partial connection and the lower λ_0 were necessary to create this overlap. For an even lower λ_0, an overlap emerged spontaneously, with a randomly selected assembly,

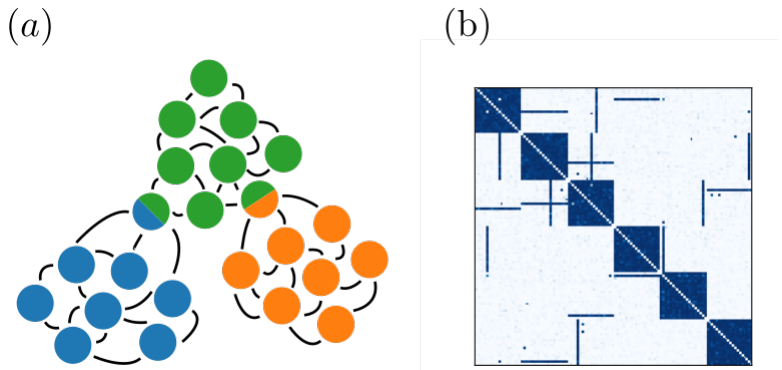

Fig 5. Overlapping assemblies. (a): Illustration of overlaps. (b): Weight matrix of a network with overlapping assemblies. The base assemblies (diagonal blocks) are each 20 neurons in size.

through the inherent stochasticity of the dynamics, as shown in Fig. 6b.

A second way of sustaining overlaps, is by having most, or all neurons be part of more than one assembly. In this case fusion of two assemblies appears less likely, because all assemblies and neurons are similarly saturated. Indeed, in the brain, we expect most

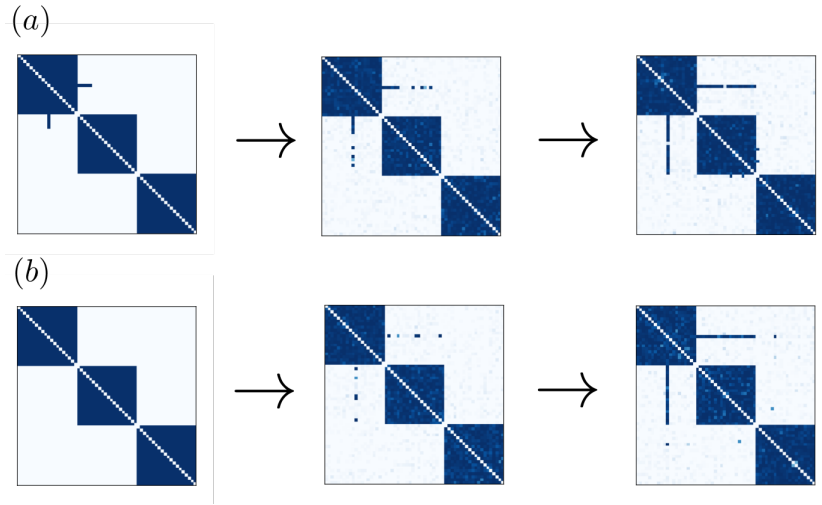

Fig 6. Creation of overlaps. (a): A partial overlap self-completes over time due to plasticity. (b): An overlap emerges for a neuron with lower spontaneous firing rate.

or all neurons to be part of more than one assembly [21, 44]. To test whether our networks are capable of sustaining similarly prominent overlap structures, we consider a network of intertwined assemblies in which each neuron is part of exactly two assemblies. We choose equally sized assemblies of size n_A and the overlap structure such that for any given assembly each of its neurons is shared with a different assembly. In other words, the overlap between any two assemblies consists of one neuron or a fraction of $1/n_A$ of the population. This implies that there are in total $n_A + 1$ assemblies and that the setup requires a network with $N = n_A(n_A + 1)/2$ neurons. Notably, a network with the same number and size of assemblies, where each neuron is only part of one assembly (no overlap), would require twice as many, $(n_A + 1)n_A$, neurons. Fig. 7 shows that this structure is stable under the STDP rule over long timescales. The assemblies have size $n_A = 19$; the typical overlap between two assemblies is thus $1/n_A = 1/19 \approx 5.3\%$.

Random correlations cause additional, extra-assembly connections to appear (more precisely: to strengthen) and intra-assembly connections to disappear (to weaken). To demonstrate that these deviations of individual weights are transient, we have tracked in Fig. 7b and c the strengthening of extra-assembly weights and the weakening of intra-assembly weights, respectively. The upper panel of Fig. 7b displays the sum of the extra-assembly weights over time, indicating that there is no positive drift, i.e. no overall increase of weights that do not belong to the stored assembly structure over time. The lower panel displays the Pearson correlations of the extra-assembly weights over time with the extra-assembly weights observed at five reference time points. With increasing distance to the reference time point, the correlations decay to chance level showing that no persistent pattern of strengthened extra-assembly weights emerges. Fig. 7c analogously displays the differences between the maximal (optimal) and the actual intra-assembly weights. The upper panel shows that there is no overall increase of this difference, i.e. no overall decay of the assembly structure. The lower panel shows that the patterns of weakened intra-assembly weights are transient.

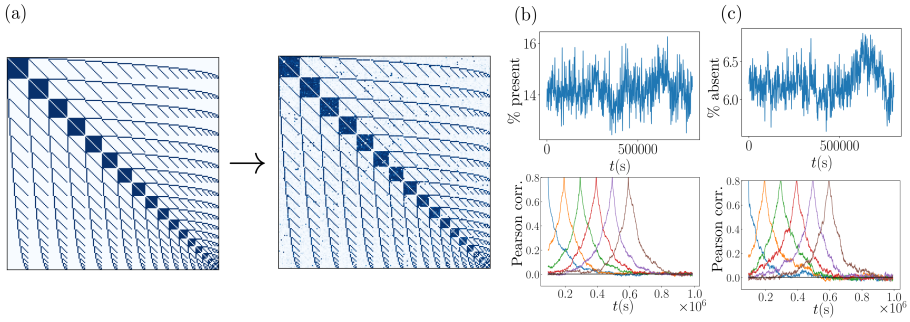

Fig 7. Intertwined assembly network. (a): Initial weight matrix (left hand side) and weight matrix after simulation over 10^6 s (right hand side). (b, upper): Sum of the extra-assembly weights, that is of those weights that are zero initially and when the assembly structure is optimally realized. The sum is given as a fraction of the total initial weights. (b, lower): Correlations of the extra-assembly weights with those at six different reference points in time. (c,upper): Sum of the absent intra-assembly weights, that is, the sum of distances of intra-assembly weights from their initial and optimal value $\hat{w}$. The sum is given as a fraction of the total initial weights. (c,lower): As in (b,lower) for absent intra-assembly weights.

Drifting assemblies

Experiments have shown that memory representations need not consist of the same neurons over time but can in fact exchange neurons without affecting behavior [25], a phenomenon called representational drift. It may occur because memory assemblies drift, by gradually exchanging neurons between each other [5]. The gradual exchange implies that at each point in time, each assembly is present and unambiguously identifiable by following the course of its evolution from the beginning. In the following, we show that our model networks can give rise to drifting assemblies. The drift happens due to two alternative mechanisms: (i) Neuron exchange between assemblies due to high weight plasticity noise, as in [5] and (ii) formation of temporal overlaps due to modulations in the spontaneous spike rate. Whether drift occurs due to mechanism (i) is chiefly determined by the learning rate μ: Fig. 8a displays the assembly dynamics in two networks with different values of μ while all other parameters are kept the same. The network with smaller μ has stationary assemblies. In contrast, the network with larger μ exhibits drifting assemblies. Specifically, in this network the ensemble of neurons

forming an assembly completely changes over time (SI Fig. S3a). Simultaneously, one can track the identity of an assembly by comparing its constituent neurons over short time intervals; the neurons forming it at one time can be unambiguously matched to the neurons forming it shortly thereafter, since the difference between those two ensembles is still small (SI Fig. S3b). We can explain the occurrence of this type of drift as an effect of fluctuations in the weight dynamics. The time-averaged weight dynamics as described by $\overline{\Delta W_{ij}}$ reinforce connections between neurons in the same assembly while suppressing connections between neurons of different assemblies. However, large enough fluctuations in the weight dynamics may nevertheless cause neurons to lose connections within their assembly and form connections to other assemblies. The size of these fluctuations is governed by μ, and if they are sufficiently large there is a finite probability that a neuron switches assemblies, see [5] for a detailed discussion. If μ is too large, the strong fluctuations prevent assemblies from forming at all.

In the second mechanism switching of assemblies by neurons is a two-step process. In the first step a neuron with a sufficiently low λ_0 spontaneously forms a connection to an additional assembly, as in Fig. 6b. Then, when λ_0 increases again this neuron loses its connections to one of the assemblies. The neuron can thereby leave either of the assemblies it is connected to – if it loses its connections to the assembly that it was originally connected to, it has switched assemblies. If this happens sufficiently often for many neurons in the network, this also causes overall drift on a slow timescale, as shown in Fig. 6b.

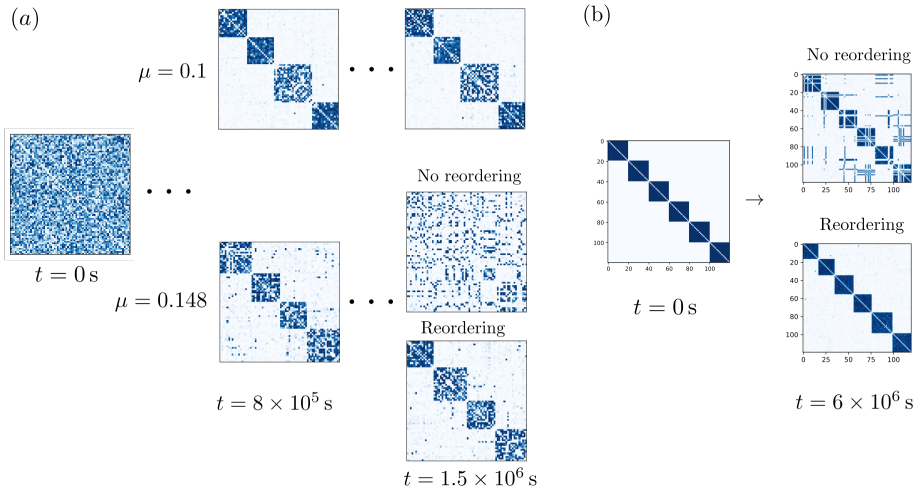

Fig 8. Drifting assemblies. (a): Drift through noisy spiking activity and resulting weight fluctuations. Assembly dynamics for lower ($\mu = 0.1$, upper part) and higher ($\mu = 0.145$, lower part) learning rate. The panel shows connection matrices W at different point in time. Initially, the weight matrices are random (left). After $t = 8 \times 10^5$ s assemblies have spontaneously emerged (middle). The neuron indices are sorted to reveal them (cf. Fig. 2). The simulation is thereafter continued, which shows that for lower learning rate the assemblies are static. In contrast, for higher learning rate the assemblies drift. Since the assemblies exchange neurons, the coupling matrix appears increasingly unstructured. Reordering of the indices, however, reveals that the assemblies are maintained at each point in time. (b): Drift through transient changes in intrinsic neuron properties and resulting transient overlaps. The spontaneous firing rates of neurons change on a slow timescale. This leads to the transient appearance of overlaps, cf. Fig. 6b. When an overlap vanishes, the neuron randomly decides for one of the assemblies, which leads to drifting assemblies.

Aging

We finally apply our assembly model to networks that undergo changes in their synaptic connectivity due to processes related to aging. Anatomical studies have shown that the aging cortex is characterized by a decrease in the number of synaptic spines [26] and presynaptic terminals [27]. These changes may be interpreted as an increase in sparsity of connections between neurons and/or as an overall weakening of synaptic strengths (since connections between neurons often consist of multiple synapses). We can model the former by permanently setting a fraction of entries of the weight matrix, chosen at random, to zero. We can model the latter by decreasing $\hat{w}$. Fig. 3a shows the effect of decreasing $\hat{w}$: it shifts the potentiation maximum and thus the typical assembly size towards larger N. Increased sparsity similarly lowers the branching parameter for an assembly of a given size and thus also shifts the potentiation maximum and the characteristic assembly size towards larger N, see Fig. 9a. As a result, spontaneously forming assemblies are larger in networks with higher sparsity, see Fig. 9c. In addition Fig. 9c suggests that smaller learning rates further increase the tendency to form larger assemblies. We observe that if the assembly sizes in a network are significantly smaller than the characteristic size predicted by Figs. 3a and 9a, assemblies will merge to form larger ones, see Fig. 9b. This represents a loss in memory capacity. Assuming that in the brain assemblies representing closely related memories merge (due to existing overlaps), during this process the overall memory content becomes less detailed and differentiated. At the same time the neuronal activity during recall increases due to larger assembly sizes indicating a less efficient use of neural resources.

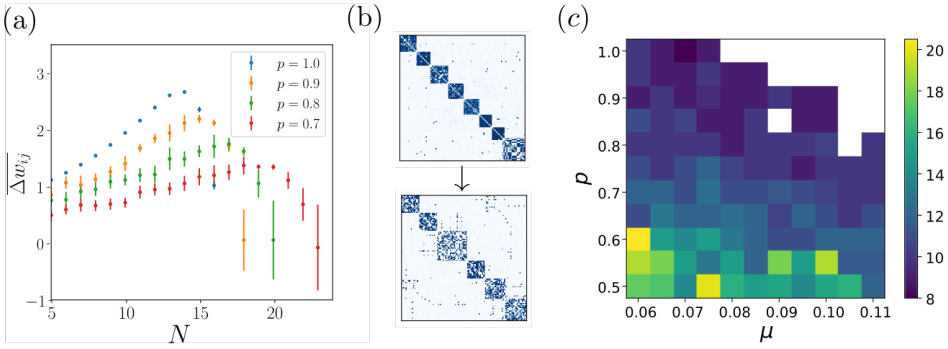

Fig 9. Effects of increasing network sparsity. (a): Time-averaged weight change like in Fig. 3a, of an assembly with intra-assembly connection probability p, as a function of its size for different values of p. Lower values of p lead to a shift of the optimal assembly size to larger N. Simulations with low $\overline{\Delta W_{ij}}$ converge slowly, which is reflected by large error bars. (b): An assembly structure becomes coarser (fewer, larger assemblies) as the connectivity sparsity increases. The panel shows the weight matrices of the same network when the probability p that a connection between neurons exists is decreased from $p = 1.0$ (upper subpanel, after spontaneous assembly emergence) to $p = 0.7$ (lower subpanel, after re-equilibration). (c): Dependence of the size of a typical assembly on the network connection probability p and the learning rate μ. The panel shows the median size of spontaneously forming assemblies in networks with random initial connectivity. White areas denote parameter regions for which activity becomes pathological, that is, firing rates diverge.

Discussion

We have studied assemblies in networks with plasticity that is purely spike-timing dependent. We find that the networks stably store assemblies, which may spontaneously emerge or be learned. Further, the assemblies can have overlaps, spontaneously drift and adapt to changing network properties.

In biological spiking neural networks the change of synaptic efficacies depends to a large extent on STDP, where depression and potentiation are a function of the time lags between pre- and postsynaptic spikes [45–47]. Assemblies may be kept up by the co-spiking of their member neurons, which strengthens their interconnections. If the total input to a neuron is not constrained, large assemblies generate large inputs to each member neuron and thereby highly reliably co-activate them. Furthermore, larger assemblies generate stronger input to other neurons and thereby tend to recruit them, such that the assembly grows. This generates a positive feedback loop, which can without restraining mechanisms lead to excessive assembly growth. Previous work on assembly networks therefore usually added additional homeostatic plasticity that limits the total input strength to a neuron by fast normalization [5, 7–9, 11–13]. This curtails the resulting excessive assembly growth. The homeostatic plasticity observed in neurobiological experiments is, however, much slower than that required to prevent runaway assembly growth [14–18].

In the present work, we therefore studied assemblies in networks with purely STDP-based plasticity. We find that our depression-dominated STDP-rule (the integral of the STDP window is negative) restricts the growth of assemblies by two mechanisms: On the one hand, the spike rate of the neurons in an assembly grows with the assembly size, which increases the depressing effect of the rate-based term of the time-averaged weight change. On the other hand, the contributions of the higher-order connectivity motifs to the time-averaged weight change become more significant the larger the assemblies are, because longer cascades of spikes become more likely. Further for sufficiently high order the appropriately summed contributions of the motifs are approximately proportional to the integral of the STDP window and thus negative. The contributions of the purely firing rate-based and the higher-order motifs therefore reduce or even invert the tendency of weights to grow in large assemblies. As a consequence, neurons are more prone to leave a larger assembly and for example join another, smaller one, which induces larger growth of the interconnecting weights. A mechanism similar to the purely firing rate-based effect that we have described has been shown to stabilize the output spike rate of a single neuron receiving feedforward input, since a strong dominance of the rate-based term ultimately leads to the reversal of the sign of plasticity [48]. Another related work, [10], demonstrated the learning of static, non-overlapping assemblies in networks with STDP in the recurrent excitatory and the inhibitory-to-excitatory connections. These assemblies are maintained at least over several hours. The excitatory STDP is thereby balanced (the integral over the STDP window is about zero) such that the inhibitory STDP is effectively much faster. This yields rate homeostasis in the excitatory neurons. In our models the integral over the excitatory STDP curve is negative. Like rate homeostasis, this restricts the maximal average excitatory spike rates. In contrast to rate homeostasis, it also allows for smaller weights, for example in our networks with assembly and background neurons. We note that the fast weight homeostasis in [9] is implemented such that it also only constrains the maximal summed input and output weight of a neuron. We further note that highly diverse average spike rates are observed in biology [49].

Our model networks generate irregular, probabilistic spiking activity. This is in agreement with experimentally observed irregular spiking in the cortex. In our models the irregularity of spiking is guaranteed by the usage of a Poisson spiking neuron model. In biological neural networks, it is usually assumed to result from the input

fluctuation-driven spiking dynamics of individual neurons, which occur when there is an overall balance of excitatory and inhibitory input. When the excitatory synaptic weights are plastic, as in our model, this balance might be maintained by inhibitory plasticity [6–8, 10].

We observe that our networks are able to maintain prominent overlap structures, where each neuron belongs to more than one assembly. The assembly structure is saturated and remains stable. In particular, additionally increased connections are sparse and transient. Previous related works have not shown similarly prominent overlap structures [5, 7–10, 12, 24], perhaps because the mostly assumed fast homeostatic normalization induces a stronger competition between the assemblies. This may force neurons to decide for one assembly. Networks with overlaps allow a more economic use of neural resources, in the sense that more assemblies of a specific size can be stored, in our example network twice as many as without overlaps. The overlap between assemblies in our simulations is about 5%. This agrees with the overlap estimated for assemblies representing associated concepts in the brain [44]. The overlap of randomly chosen assemblies is smaller, about 1%.

Our model networks can stably maintain assemblies in front of a background of neurons that are not part of any assembly. Such a scenario might be particularly relevant for early development when not many memories have been stored yet. Previous related works usually assume that the entire space is tiled by assemblies [5, 7–10, 12]. The reason may be similar as for the prominent overlap structures, namely that fast homeostatic plasticity has a strong tendency to force neurons into assemblies. Ref. [24] shows assemblies in front of a background of weakly connected neurons in networks with structural plasticity and multiple synapses per connection between neurons.

The assemblies in our networks can drift. Such assembly drift may explain the experimentally observed drift of memory representations in the brain [25]. In our model, assemblies drift by exchanging neurons. This exchange can on the one hand originate from sufficiently large synaptic weight fluctuations, as in [5]. These fluctuations occur in our models for sufficiently large learning rates due to the noisy spiking. On the other hand, our models also show a novel neuron exchange (and thus drift) mechanism: For high spontaneous rate, each neuron belongs to one assembly. If the spontaneous rate of a neuron in the network then transiently drops, the synaptic weights with another assembly increase, such that the neuron belongs to two assemblies. When the intrinsic rate recovers, the synaptic weights with one of the assemblies weaken. This may eliminate the strong weights with the assembly that the neuron originally belonged to and thus induce a switch to the other assembly. The observation suggests a new general mechanism for representational drift in the brain: Transient (or persistent) changes in single neuron properties may lead to changes in the synaptic weights. These in turn induce a change in the features represented by the neuron. The changes in the synaptic weights and the representation may thereby be much longer lasting than the changes in the intrinsic neuronal properties.

Since in the aging brain the overall connectivity decreases [26, 27], we have explored the impact of a such a decrease on the assemblies in our model networks. We observe that the size of assemblies is inversely related to the connection probability in the network. We expect that a similar relation can be observed rather generally, for example also in model networks where the assemblies are stabilized by fast homeostasis. In particular, sparser networks should, all other parameters being equal, lead to larger assemblies that are activated during recall. This is consistent with the observation that neural activity for the same task is stronger in aged individuals [50], where the neural networks are more sparsely connected. An increased assembly size and the resulting stronger activity during reactivation might also explain why episodic memories are experienced more vividly in elderly subjects [51]. In our model networks, we observe

that assemblies merge to larger ones when networks become increasingly sparse. Such mergers might explain why episodic memories become less detailed in the aging brain [51, 52].

Acknowledgments

We thank Sven Goedeke for helpful comments on the manuscript.

References

1. Buzsáki G. Neural syntax: cell assemblies, synapsembles, and readers. Neuron. 2010;68(3):362–385.
2. Gerstner W, Kistler WM, Naud R, Paninski L. Neuronal dynamics: From single neurons to networks and models of cognition. Cambridge University Press; 2014.
3. Holtmaat A, Caroni P. Functional and structural underpinnings of neuronal assembly formation in learning. Nat Neurosci. 2016;19(12):1553.
4. Pietri T, Romano SA, Pérez-Schuster V, Boulanger-Weill J, Candat V, Sumbre G. The emergence of the spatial structure of tectal spontaneous activity is independent of visual inputs. Cell Rep. 2017;19(5):939–948.
5. Kossio YFK, Goedeke S, Klos C, Memmesheimer RM. Drifting assemblies for persistent memory: Neuron transitions and unsupervised compensation. Proc Natl Adac Sci U S A. 2021;118(46).
6. Vogels TP, Sprekeler H, Zenke F, Clopath C, Gerstner W. Inhibitory plasticity balances excitation and inhibition in sensory pathways and memory networks. Science. 2011;334(6062):1569–1573.
7. Litwin-Kumar A, Doiron B. Formation and maintenance of neuronal assemblies through synaptic plasticity. Nat Commun. 2014;5(1):1–12.
8. Zenke F, Agnes EJ, Gerstner W. Diverse synaptic plasticity mechanisms orchestrated to form and retrieve memories in spiking neural networks. Nat Commun. 2015;6(1):1–13.
9. Ravid Tannenbaum N, Burak Y. Shaping neural circuits by high order synaptic interactions. PLoS Comput Biol. 2016;12(8):e1005056.
10. Ocker GK, Doiron B. Training and spontaneous reinforcement of neuronal assemblies by spike timing plasticity. Cereb Cortex. 2019;29(3):937–951.
11. Herpich J, Tetzlaff C. Principles underlying the input-dependent formation and organization of memories. Netw Neurosci. 2019;3(2):606–634.
12. Montangie L, Miehl C, Gjorgjieva J. Autonomous emergence of connectivity assemblies via spike triplet interactions. PLoS Comput Biol. 2020;16(5):e1007835.
13. Triplett MA, Avitan L, Goodhill GJ. Emergence of spontaneous assembly activity in developing neural networks without afferent input. PLoS Comput Biol. 2018;14(9):e1006421.
14. Huang YY, Colino A, Selig DK, Malenka RC. The influence of prior synaptic activity on the induction of long-term potentiation. Science. 1992;255(5045):730–733.

15. Turrigiano GG, Leslie KR, Desai NS, Rutherford LC, Nelson SB. Activity-dependent scaling of quantal amplitude in neocortical neurons. Nature. 1998;391(6670):892–896.

16. Ibata K, Sun Q, Turrigiano GG. Rapid synaptic scaling induced by changes in postsynaptic firing. Neuron. 2008;57(6):819–826.

17. Zenke F, Gerstner W, Ganguli S. The temporal paradox of Hebbian learning and homeostatic plasticity. Curr Opin Neurobiol. 2017;43:166–176.

18. Zenke F, Gerstner W. Hebbian plasticity requires compensatory processes on multiple timescales. Philos Trans R Soc Lond B Biol Sci. 2017;372(1715):20160259.

19. Tetzlaff C, Kolodziejski C, Timme M, Wörgötter F. Synaptic scaling in combination with many generic plasticity mechanisms stabilizes circuit connectivity. Front Comput Neurosci. 2011;5:47.

20. Lagzi F, Bustos MC, Oswald AM, Doiron B. Assembly formation is stabilized by Parvalbumin neurons and accelerated by Somatostatin neurons. bioRxiv. 2021;.

21. De Falco E, Ison MJ, Fried I, Quiroga RQ. Long-term coding of personal and universal associations underlying the memory web in the human brain. Nat Commun. 2016;7(1):1–11.

22. Rey HG, De Falco E, Ison MJ, Valentin A, Alarcon G, Selway R, et al. Encoding of long-term associations through neural unitization in the human medial temporal lobe. Nat Commun. 2018;9(1):1–13.

23. Rey HG, Gori B, Chaure FJ, Collavini S, Blenkmann AO, Seoane P, et al. Single neuron coding of identity in the human hippocampal formation. Curr Biol. 2020;30(6):1152–1159.

24. Fauth MJ, van Rossum MC. Self-organized reactivation maintains and reinforces memories despite synaptic turnover. Elife. 2019;8. doi:10.7554/elife.43717.

25. DeNardo LA, Liu CD, Allen WE, Adams EL, Friedmann D, Fu L, et al. Temporal evolution of cortical ensembles promoting remote memory retrieval. Nat Neurosci. 2019;22(3):460–469.

26. Feldman ML, Dowd C. Loss of dendritic spines in aging cerebral cortex. Anat Embryol (Berl). 1975;148(3):279–301.

27. Masliah E, Mallory M, Hansen L, DeTeresa R, Terry R. Quantitative synaptic alterations in the human neocortex during normal aging. Neurology. 1993;43(1 Part 1):192–192.

28. Van Vreeswijk C, Sompolinsky H. Chaos in neuronal networks with balanced excitatory and inhibitory activity. Science. 1996;274(5293):1724–1726.

29. Kempter R, Gerstner W, Van Hemmen JL. Hebbian learning and spiking neurons. Phys Rev E. 1999;59(4):4498.

30. Pernice V, Staude B, Cardanobile S, Rotter S. How Structure Determines Correlations in Neuronal Networks. PLoS Comput Biol. 2011;7(5):e1002059. doi:10.1371/journal.pcbi.1002059.

31. Kalle Kossio YF, Goedeke S, van den Akker B, Ibarz B, Memmesheimer RM. Growing Critical: Self-Organized Criticality in a Developing Neural System. Phys Rev Lett. 2018;121:058301. doi:10.1103/PhysRevLett.121.058301.

32. Gerstein GL, Mandelbrot B. Random walk models for the spike activity of a single neuron. Biophys J. 1964;4(1):41–68.

33. Shadlen MN, Newsome WT. Noise, neural codes and cortical organization. Curr Opin Neurobiol. 1994;4(4):569–579.

34. Jahnke S, Memmesheimer RM, Timme M. Stable irregular dynamics in complex neural networks. Phys Rev Lett. 2008;100(4):048102.

35. Denève S, Machens CK. Efficient codes and balanced networks. Nat Neurosci. 2016;19:375–382. doi:10.1038/nn.4243.

36. Manz P, Goedeke S, Memmesheimer RM. Dynamics and computation in mixed networks containing neurons that accelerate towards spiking. Phys Rev E. 2019;100(4):042404.

37. Hawkes AG. Spectra of some self-exciting and mutually exciting point processes. Biometrika. 1971;58(1):83–90.

38. Hawkes AG. Point spectra of some mutually exciting point processes. J R Stat Soc Series B Stat Methodol. 1971;33(3):438–443.

39. Mishra RK, Kim S, Guzman SJ, Jonas P. Symmetric spike timing-dependent plasticity at CA3–CA3 synapses optimizes storage and recall in autoassociative networks. Nat Commun. 2016;7(1):1–11.

40. Yun R, Mishler JH, Perlmutter SI, Fetz EE. Paired stimulation for spike-timing dependent plasticity quantified with single neuron responses in primate motor cortex. bioRxiv. 2022;.

41. Dayan P, Abbott LF. Theoretical neuroscience: computational and mathematical modeling of neural systems. MIT press; 2005.

42. Harris TE, et al. The theory of branching processes. vol. 6. Springer Berlin; 1963.

43. Beggs JM, Plenz D. Neuronal avalanches in neocortical circuits. J Neurosci. 2003;23(35):11167–11177.

44. Gastaldi C, Schwalger T, De Falco E, Quiroga RQ, Gerstner W. When shared concept cells support associations: Theory of overlapping memory engrams. PLoS Comput Biol. 2021;17(12):e1009691.

45. Dan Y, Poo Mm. Spike timing-dependent plasticity of neural circuits. Neuron. 2004;44(1):23–30.

46. Caporale N, Dan Y. Spike timing–dependent plasticity: a Hebbian learning rule. Annu Rev Neurosci. 2008;31:25–46.

47. Ziv NE, Brenner N. Synaptic tenacity or lack thereof: spontaneous remodeling of synapses. Trends Neurosci. 2018;41(2):89–99.

48. Kempter R, Gerstner W, Hemmen JLv. Intrinsic stabilization of output rates by spike-based Hebbian learning. Neural Comput. 2001;13(12):2709–2741.

49. Buzsáki G, Mizuseki K. The log-dynamic brain: how skewed distributions affect network operations. Nat Rev Neurosci. 2014;15(4):264–278. doi:10.1038/nrn3687.

50. Spaniol J, Grady C. Aging and the neural correlates of source memory: over-recruitment and functional reorganization. Neurobiol Aging. 2012;33(2):425–e3.

51. Folville A, Simons JS, D'Argembeau A, Bastin C. I remember it like it was yesterday: Age-related differences in the subjective experience of remembering. Psychon Bull Rev. 2021;doi:10.3758/s13423-021-02048-y.

52. Levine B, Svoboda E, Hay JF, Winocur G, Moscovitch M. Aging and autobiographical memory: Dissociating episodic from semantic retrieval. Psychol Aging. 2002;17(4):677–689. doi:10.1037/0882-7974.17.4.677.